

# The anomalous production of multi-leptons and its impact on the measurement of $Wh$ production at the LHC

Yesenia Hernandez,<sup>1,\*</sup> Alan S. Cornell,<sup>2,†</sup> Mukesh Kumar,<sup>1,‡</sup> Bruce Mellado,<sup>1,3,§</sup> and Xifeng Ruan<sup>1,¶</sup>

<sup>1</sup>*School of Physics and Institute for Collider Particle Physics,  
University of the Witwatersrand, Johannesburg, Wits 2050, South Africa.*

<sup>2</sup>*Department of Physics, University of Johannesburg,  
PO Box 524, Auckland Park 2006, South Africa.*

<sup>3</sup>*iThemba LABS, National Research Foundation, PO Box 722, Somerset West 7129, South Africa.*

Statistically compelling anomalies in multi-lepton final states at the Large Hadron Collider, LHC, have been reported in Refs. [1, 2]. These can be interpreted in terms of the production of a heavy boson,  $H$ , decaying into a Standard Model (SM) Higgs boson,  $h$ , and a singlet scalar,  $S$ , which is treated as a SM Higgs-like boson, where  $m_H \approx 270$  GeV and  $m_S \approx 150$  GeV. This process would affect the measurement of the  $Wh$  signal strength at the LHC, where  $h$  is produced in association with leptons and di-jets. Here,  $h$  would be produced with lower transverse momentum,  $p_{T_h}$ , compared to the SM process. Provided that no stringent requirements are made on  $p_{T_h}$ , the signal strength of  $Wh$  is  $\mu(Wh) = 2.51 \pm 0.43$ , which corresponds to a deviation from the SM of  $3.5\sigma$ . This result further enriches the plethora of multi-lepton anomalies at the LHC. If confirmed with more Run 2 data, this result would indicate that the Higgs boson produced at the LHC is contaminated with production mechanisms other than in the SM. In turn, this compromises the ability of high energy proton-proton collisions to gain access to the couplings of the Higgs boson to SM particles in a model-independent way, as opposed to  $e^+e^-$  and to, a less extent,  $e^-p$  collisions.

## I. INTRODUCTION

The discovery of a Higgs boson ( $h$ ) [3–6] at the Large Hadron Collider (LHC) by the ATLAS [7] and CMS [8] experiments has opened a new chapter in particle physics. Measurements provided so far indicate that the quantum numbers of this boson are consistent with those predicted by the Standard Model (SM) [9, 10], and that the relative branching ratios (BRs) to SM particles follow what is predicted by the SM. With this in mind, a window of opportunity now opens for the search for new bosons and how these would affect the  $h$  boson measurements. The first hints towards the establishment of new heavier bosons were given in Refs. [11, 12], where a number of features in data taken during the Run 1 period of the LHC, including but not limited to some  $h$ -related measurements, were investigated. These were embedded into a 2HDM+S extension of the SM, where  $S$  is an electroweak (EW) singlet [12, 13]. If the hints reported in Refs. [11, 12] are indeed due to the presence of additional bosons, significant excesses could be found in the LHC data in multi-lepton final states. Significant excesses were first reported in Ref. [1], where Ref. [2] and subsequent results [14] have demonstrated that the significance of the multi-lepton excesses is now large enough to exclude these effects being due to statistical fluctuations. A simplified 2HDM+S [12, 13] model, where the

dominance of the decay  $H(270) \rightarrow S(150)h(125)^1$  is assumed, is able to capture a wide range of excesses that include opposite sign di-leptons, same-sign di-leptons, and three leptons, with and without the presence of  $b$ -tagged hadronic jets. These are final states with vastly different cross-sections that a simple hypothesis seems to be able to describe within existing errors. The excesses reported in Refs. [1, 2, 14] are the result of the exploration of final states where the parameters were fixed previously in Ref. [12]. Recall that the parameters of the simplified model were fixed excepting the size of the  $H$  Yukawa coupling to the top quark, with excesses observed with Run 1 data. Therefore, the large significance reported in Ref. [2] is unencumbered by phase-space and parameter “look elsewhere” effects.

Assuming the dominance  $H \rightarrow Sh$  and  $S$  behaving like a SM Higgs-like boson,  $H$  would need to be produced with a cross-section of  $\mathcal{O}(10)$  pb in proton-proton collisions with a center of mass of  $\sqrt{s} = 13$  TeV. This cross-section is large enough to significantly impact measurements of  $h$  at the LHC. The potential impact can be ameliorated by considering scenarios where the mass of  $H$  be less than the sum of the mass of  $h$  and  $S$ ,  $m_H < m_S + m_h$  or by reducing the coupling of  $h$  to SM particles [15], or a combination of both. Another option is to consider a large branching ratio of  $H \rightarrow SS$ , as opposed to  $H \rightarrow Sh$ , which could also be used to describe the multi-lepton excesses reported in Refs. [1, 2, 11] without strongly affecting the production of  $h$  with decay channels where the  $h$  mass can be reconstructed (e.g.,  $\gamma\gamma$  and  $ZZ \rightarrow 4\ell$ ,  $\ell = e, \mu$ ).

\* yesenia@cern.ch

† acornell@uj.ac.za

‡ mukesh.kumar@cern.ch

§ bmellado@mail.cern.ch

¶ xifeng.ruan@cern.ch

<sup>1</sup> Here,  $H, S, h$  correspond to mass ordered scalars in the 2HDM+S model.

In Ref. [16] the impact on the measurement of the process  $H \rightarrow Sh$  was evaluated in final states including  $h \rightarrow \gamma\gamma$  in association with hadronic jets. In particular, it was demonstrated that the impact on the measurement of  $h$  produced via Vector Boson Fusion (VBF) would be moderate, where the measurement of  $h$  in association with  $W \rightarrow jj$  would be affected significantly, as long as the transverse momentum of  $h$ ,  $p_{Th} < m_W$ , where  $m_W$  is the mass of the  $W$  boson.

In this article we expand on Ref. [16] by studying the potential impact on measurements related to  $Wh, W \rightarrow jj\ell\nu, \ell = e, \mu$  and other relevant final states used in the measurement of the signal strength of  $Wh$  by the LHC experiments. A survey of the existing measurements of the cross-section of the  $Wh$  production mechanism from the ATLAS and CMS experiments is performed, with emphasis on measurements of the signal strength of the  $Wh$  production mechanism in the corner of the phase space where  $p_{Th} < m_W$  is explored. Here we evaluate the size of the deviation from the SM in the production of  $Wh$ , as measured by the LHC experiments. The final states considered here were not included in the statistical analyses reported in Refs. [1, 2].

The paper is organized as follows: Section II succinctly describes the simplified model used to model the BSM signal described above; Section III reports on the available data and the methodology used to study it; Section IV summarizes the findings of the paper and quantifies the size of the observed anomaly in the Higgs boson data.

## II. THE SIMPLIFIED MODEL

In Refs. [11, 12] the authors postulated the existence of two new scalar bosons,  $H$  and  $S$ , where effective interaction vertices were defined. This was further extended by utilizing a two Higgs doublet model with the addition of a singlet scalar. This was dubbed the 2HDM+S, where the model's implications were used in analyzing multi lepton data [13]. In this article we have fixed the masses of  $H$  and  $S$  with the benchmark values of  $m_H = 270$  GeV and  $m_S = 150$  GeV, as determined by the best-fit values obtained from previous studies [1, 11]. It should be noted, however, that many of the results used to constrain the masses arise from the non-resonant production of multiple leptons to begin with, and so the distributions that were used to fit the simplified model were not always significantly sensitive to the masses of the heavy scalars (at least up to a variation of a few tens of GeV).

In terms of interactions,  $H$  is assumed to be linked to EW symmetry breaking, in that it has Yukawa couplings. The simplified Lagrangian used to describe the production of  $H$  is:

$$\mathcal{L}_H = -\frac{1}{4} \beta_g \kappa_{hgg}^{\text{SM}} G_{\mu\nu} G^{\mu\nu} H + \beta_V \kappa_{hVV}^{\text{SM}} V_\mu V^\mu H. \quad (1)$$

These are the effective vertices required so that  $H$  couples

to gluons and the heavy vector bosons  $V = W^\pm, Z$ , respectively. The first term in Eq. (1) allows for the gluon fusion ( $ggF$ ) production mode of  $H$ , while the second term describes the VBF production mode of  $H$ . The  $\kappa_{hgg}^{\text{SM}}$  and  $\kappa_{hVV}^{\text{SM}}$  are the effective coefficients for the equivalent SM Higgs gluon fusion, and Higgs vector-boson fusion, whilst  $\beta_g = y_{tH}/y_{tth}$  is the scale factor with respect to the SM Yukawa top coupling for  $H$ , and it is therefore used to tune the effective  $ggF$  coupling. A similar factor  $\beta_V$  is used for  $VVH$  couplings.

The  $S$  boson, on the other hand, is assumed to not be produced directly, but rather through the decay of  $H$ . In principle, it is possible to include  $S$  as a singlet scalar that has interactions with  $H$  and the SM Higgs boson  $h$ . Doing this would allow the  $H$  to produce  $S$  bosons through the  $H \rightarrow SS$  and  $Sh$  decay modes. Here, we assume the  $H \rightarrow Sh$  decay mode to have a 100% BR. These assumptions are all achieved by introducing the following effective interaction Lagrangians:

- Firstly,  $S$  is given a vacuum expectation value and couples to the scalar sector,

$$\mathcal{L}_{HhS} = -\frac{1}{2} v \left[ \lambda_{hhs} hhS + \lambda_{hSS} hSS + \lambda_{HHS} HHS + \lambda_{HSS} HSS + \lambda_{HhS} HhS \right], \quad (2)$$

where the couplings are fixed to ensure that the  $H \rightarrow Sh$  BR is 100%.

- Secondly,  $S$  is given Higgs-like BRs by fixing the parameters in the Lagrangian,

$$\begin{aligned} \mathcal{L}_S = & \frac{1}{4} \kappa_{Sgg} \frac{\alpha_s}{12\pi v} SG^{a\mu\nu} G_{\mu\nu}^a + \frac{1}{4} \kappa_{S\gamma\gamma} \frac{\alpha}{\pi v} SF^{\mu\nu} F_{\mu\nu} \\ & + \frac{1}{4} \kappa_{SZZ} \frac{\alpha}{\pi v} SZ^{\mu\nu} Z_{\mu\nu} + \frac{1}{4} \kappa_{SZ\gamma} \frac{\alpha}{\pi v} SZ^{\mu\nu} F_{\mu\nu} \\ & + \frac{1}{4} \kappa_{Sww} \frac{2\alpha}{\pi s_w^2 v} SW^{+\mu\nu} W_{\mu\nu}^- - \sum_f \kappa_{Sff} \frac{m_f}{v} S\bar{f}f. \end{aligned} \quad (3)$$

Additionally, the couplings are globally re-scaled in order to suppress the direct production of  $S$ .

Fixing the BRs of  $S$  reduces the number of free parameters in the model. For simplicity the BRs of  $S$  are set to the same as that of a SM Higgs boson in the mass range considered here. In the above Lagrangian,  $W_{\mu\nu}^\pm = D_\mu W_\nu^\pm - D_\nu W_\mu^\pm$ , and similarly  $Z_{\mu\nu} = D_\mu Z_\nu - D_\nu Z_\mu$ , and  $F_{\mu\nu}$  is the usual electromagnetic field strength tensor. The covariant derivative is defined as  $D_\mu W_\nu^\pm = [\partial_\mu \pm ieA_\mu] W_\nu^\pm$ . Other possible self interaction terms for  $S$  are neglected here, since they are not of any phenomenological interest for our studies.

## III. METHODOLOGY

The production of  $h$  in association with  $W$  through Drell-Yan processes provides the distinct feature that  $h$  is

produced with large transverse momentum ( $p_{Th}$ ). A significantly large rate of  $h$  can be produced with  $p_{Th} > m_W$  where backgrounds can be strongly suppressed. This is actively used by the LHC experiments to isolate corners of the phase-space, where the  $h$  signal can be effectively extracted for measurements of the signal strength. This implies that searches and measurements of  $Wh$  at the LHC give preference to regions of the phase-space with  $p_{Th} > m_W$ , a considerable bias if one is looking for deviations from the SM in the Higgs sector. This is achieved either by truncating the phase-space, excluding low  $p_{Th}$  with large backgrounds, or by implementing multivariate analyses that include observables sensitive to  $p_{Th}$ , where the relative weight of large transverse momentum production is enhanced.

By contrast, with the BSM signal  $H(270) \rightarrow S(150)h(125)$ ,  $h$  displays significantly lower transverse momentum [12]. To a considerable degree, the  $h$  signal produced via SM and BSM production mechanisms appears adjacent, but are distinct regions of the phase-space. The results provided by the ATLAS and CMS experiments pertain to the search and measurement of  $Wh$  production in the SM and are not optimal for the search for new physics in general, and the BSM signal considered here, in particular. Nonetheless, a straw man approach is adopted here whereby results that rely heavily on  $p_{Th}$ , or correlated observables, are discarded. Those results that explore the phase-space more “inclusively” are considered here instead.

The experimental results reviewed here pertain to searches and measurements of  $Wh$  in the SM, where the preferred phase-space is identified based on the SM itself. Therefore, in the presence of potential admixtures of BSM via the production of  $h$  through production mechanisms other than those in the BSM, measurements of the  $Wh$  signal strength would be naturally biased towards unity. Even in those cases where the measurement is performed more “inclusively” (i.e. without the application of stringent requirements on  $p_{Th}$ ), results are obtained by weighting the phase-space according to how the SM populates it. The size of the bias is model dependent and it is not studied here. The discussion regarding the conservativeness of the results reported in Section IV remains qualitative.

Table I summarizes the results from ATLAS and CMS experiments for the SM Higgs boson produced to date in association with a  $W$  boson in leptonic and di-jet final states. The Higgs decay modes considered here include  $h \rightarrow WW, \tau\tau, \gamma\gamma$ . In the following the main event selection for each analysis is briefly described and the motivation for including or excluding results in the combination reported in Section IV is discussed.

#### A. $Vh \rightarrow VWW$

The  $Wh$  results in the  $h \rightarrow WW^*$  decay using the Run 1 data sample collected at the ATLAS detector are ob-

tained in two- and three-lepton final states [17], denoted in the following as  $2\ell$  and  $3\ell$ , respectively. The former requires exactly two well isolated leptons with high transverse momentum and is further split in different-flavor opposite-sign (DFOS) and same-sign (SS)  $2\ell$  channels.

In the DFOS  $2\ell$  category the vectorial boson (either a  $W$  or  $Z$  boson) associated to the Higgs boson decays hadronically and produces two jets, while the  $e^\pm\mu^\mp$  pair originates from the  $h \rightarrow WW^*$  process. The SS  $2\ell$  channel targets  $Wh$  production when the  $W$  boson that radiates the Higgs boson decays leptonically, while one of the  $W$  bosons coming from  $h \rightarrow WW^*$  decays hadronically, and the other - with same charge as the former  $W$  boson - decays leptonically. In both categories lower bounds on the invariant mass of the lepton pair ( $m_{\ell\ell}$ ) and on the missing transverse energy ( $E_T^{\text{miss}}$ ) are applied, as well as a veto on events with the presence of  $b$ -tagged jets. For DFOS  $2\ell$  events, several constraints on the dijet kinematics are required to select jets associated to  $W/Z$  bosons. The rapidity separation between the two highest  $p_T$  jets,  $\Delta y_{jj} < 1.2$ , and the invariant mass of these two jets,  $|m_{jj} - 85| < 15$  GeV, are imposed. Finally, the selection exploits the kinematics of the lepton pair to be consistent with the  $h \rightarrow WW^*$  decay, so the azimuthal angular separation between the two leptons ( $\Delta\phi_{\ell\ell}$ ) is required to be below 1.8 rad and  $m_{\ell\ell} < 50$  GeV. In the SS  $2\ell$  channel a further categorization divides the events by having exactly one jet or exactly two jets in the final state. Similarly to the DFOS category, a set of requirements on the minimum invariant mass of a lepton and a jet, the smallest opening angle between the lepton which minimizes the above variable and a jet, and the transverse mass of the leading lepton and the  $E_T^{\text{miss}}$  ( $m_T$ ) are used. All these channels present an observed signal strength which is above the unity in one to two standard deviations ( $\sigma$ ), as observed in Table I. The measured signal strength of the  $2\ell$  categories in ATLAS using Run 1 data results in  $3.7_{-1.5}^{+1.9}$  [17]. This result will be used in the combination of the ATLAS and CMS  $Vh$  observed signal strength in this paper.

In the  $3\ell$  channel the  $W$  bosons are expected to decay leptonically. These events are selected by having exactly three leptons with total charge of  $\pm 1$  and at most one jet in the final state. Events are further categorized depending on the presence of same-flavor opposite-sign (SFOS) lepton pairs: 0SFOS and 1SFOS. The 0SFOS category includes  $e^\pm e^\pm \mu^\mp$  and  $\mu^\pm \mu^\pm e^\mp$  final states. These types of events highly benefit from low background contamination and no additional selection is applied. The angular separation of the Higgs decay lepton candidates ( $\Delta R_{\ell\ell}$ ) is used in the likelihood fit to extract the results. The observed signal strength of the 0SFOS category is  $1.7_{-1.4}^{+1.9}$  and it will be considered in the results section. Events with at least 1SFOS lepton pair require  $\Delta R_{\ell\ell} < 2$  and the invariant mass of all SFOS combinations must satisfy  $|m_{\ell^\pm \ell^\mp} - m_Z| > 25$  GeV in order to reject  $WZ$  and  $ZZ$  events. In addition, a multivariate discriminant based on Boosted Decision Trees (BDT) [28, 29] is used. An im-

TABLE I. Summary of ATLAS and CMS  $Vh$  results.

Higgs decay	Ref.	Experiment	$\sqrt{s}, \mathcal{L}$ TeV, fb $^{-1}$	Final state	Category	$\mu$	Used in combination	Comments
	[17]	ATLAS	7, 4.5 8, 20.3	$2\ell$	DFOS 2j	$2.2^{+2.0}_{-1.9}$	✓	$2\ell$ combination: $\mu = 3.7^{+1.9}_{-1.5}$  $m_{\ell_0\ell_2}$ used as input BDT discriminating variable
					SS 1j	$8.4^{+4.3}_{-3.8}$	✓	
					SS 2j	$7.6^{+6.0}_{-5.4}$	✓	
					1SFOS	$-2.9^{+2.7}_{-2.1}$	x	
					0SFOS	$1.7^{+1.9}_{-1.4}$	✓	
WW	[18]	ATLAS	13, 36.1	$3\ell$	1SFOS	$2.3^{+1.2}_{-1.0}$	✓	1SFOS channel uses $m_{\ell_0\ell_2}$ in the BDT but excess driven by 0SFOS
					0SFOS			
	[19]	CMS	7, 4.9 8, 19.4	$2\ell$	DFOS 2j	$0.39^{+1.97}_{-1.87}$	✓	Discrepancy at low $m_{\ell\ell}$
					$0+1$ SFOS	$0.56^{+1.27}_{-0.95}$	✓	
[20]	CMS	13, 35.9	$2\ell$	DFOS 2j	$3.92^{+1.32}_{-1.17}$	✓	Discrepancy at low $m_{\ell\ell}$	
				$0+1$ SFOS	$2.23^{+1.76}_{-1.53}$	✓		
$\tau\tau$	[21]	ATLAS	8, 20.3	$1\ell$	$\ell + \tau_h\tau_h$	$1.8 \pm 3.1$	✓	BDT based on $p_T^{\tau_1} + p_T^{\tau_2}$ Split $p_T^{\ell_1} + p_T^{\ell_2} + p_T^{\tau}$ at 130 GeV
				$2\ell$	$e^\pm\mu^\pm + \tau_h$	$1.3 \pm 2.8$	✓	
	[22]	CMS	7, 4.9 8, 19.7	$1\ell$	$\ell + \tau_h\tau_h$	$-0.33 \pm 1.02$	x	
				$2\ell$	$e^\pm\mu^\pm + \tau_h$		x	
	[23]	CMS	13, 35.9	$1\ell$	$\ell + \tau_h\tau_h$	$3.39^{+1.68}_{-1.54}$	✓	
				$2\ell$	$e^\pm\mu^\pm + \tau_h$			
$\gamma\gamma$	[24]	ATLAS	7, 5.4 8, 20.3	$\ell\nu$	one-lepton	$1.0 \pm 1.6$	x	$E_T^{\text{miss}} > 70 - 100$ GeV $p_T^{\gamma\gamma} > 70$ GeV
				$\cancel{\nu}, \nu\nu$	$E_T^{\text{miss}}$			
	[25]	CMS	7, 5.1 8, 19.7	$\ell\nu$	one-lepton	$-0.16^{+1.16}_{-0.79}$	x	Split $E_T^{\text{miss}}$ at 45 GeV $E_T^{\text{miss}} > 70$ GeV $p_T^{\gamma\gamma} > 13m_{\gamma\gamma}/12$
				$\cancel{\nu}, \nu\nu$	$E_T^{\text{miss}}$			
[26]	ATLAS	13, 36.1	$\ell\nu$	one-lepton	$0.7^{+0.9}_{-0.8}$	x	$p_T^{\ell+E_T^{\text{miss}}} > 150$ GeV $p_T^{\ell+E_T^{\text{miss}}} < 150$ GeV $150 < E_T^{\text{miss}} < 250$ GeV $80 < E_T^{\text{miss}} < 150$ GeV	
			$\cancel{\nu}, \nu\nu$	$E_T^{\text{miss}}$				
[27]	CMS	13, 35.6	$\ell\nu$	one-lepton	$2.4^{+1.1}_{-1.0}$	x	Split $E_T^{\text{miss}}$ at 45 GeV ( $\mu = 3.0^{+1.5}_{-1.3}$ ) $E_T^{\text{miss}} > 85$ GeV	
			$\cancel{\nu}, \nu\nu$	$E_T^{\text{miss}}$				
				$jj$	Hadronic		✓	BDT used based on $m_{jj}$ and $p_T^{\gamma\gamma}$
				$jj$	Hadronic		✓	$p_T^{\gamma\gamma}/m_{\gamma\gamma}$ not used ( $\mu = 5.1^{+2.5}_{-2.3}$ )

portant BDT input discriminating variable is the invariant mass of the lepton with different electric charge and the lepton originated from the  $W$  boson radiating the SM Higgs particle ( $m_{\ell_0\ell_2}$ ). This quantity tends to lower values for  $H \rightarrow Sh$  events compared with the  $Wh$  process as

shown in Figure 1. The same behavior is also observed for  $WZ^*$  and  $Z$ +jets events. These are the dominant background contributions for this category and they are mostly located in the  $m_{\ell_0\ell_2} < 100$  GeV region. Given this feature, it is expected that the BDT discriminates

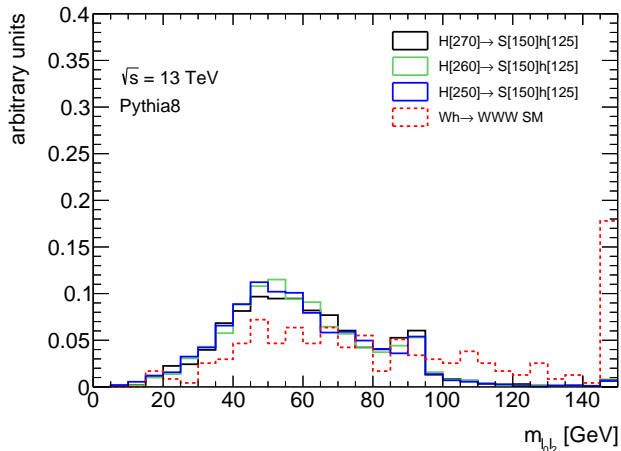


FIG. 1. Invariant mass of the lepton with different electric charge and the lepton originating from the  $W$  boson radiating the SM Higgs particle in the  $Wh\ 3\ell$  channel for several  $H \rightarrow Sh$  samples (solid lines) compared with the SM  $Vh$  process with  $h \rightarrow WW$  (dashed line) generated with PYTHIA8. The last bin contains overflow events.

these SM background processes, as well as the  $H \rightarrow Sh$  signal, in benefit of the target decay:  $Wh \rightarrow WWW$ . In light of this, the observed signal strength in 1SFOS events will not be combined with results from other categories.

ATLAS has also published more recent  $Wh$  results using  $36.1\ \text{fb}^{-1}$  from the Run 2 dataset [18] for which only  $3\ell$  channels are considered. The selection strategy follows that from Run 1, but the usage of multivariate techniques has also been extended to the 0SFOS channel. In this case two BDTs are developed to reject  $WZ$  and  $t\bar{t}$  events. Mostly leptonic kinematic variables are used as inputs to the BDT against  $WZ$  backgrounds in the 0SFOS category from which only three are common to the 1SFOS category: the invariant mass of the Higgs lepton candidates,  $E_T^{\text{miss}}$  and the difference in pseudorapidity between the leptons with the same electric charge. The BDT against  $t\bar{t}$  uses as input variables hadronic quantities such as the number of jets and the transverse momentum of the jet with highest  $p_T$ . The observed signal strength combining all  $3\ell$  channels shows a deviation of about  $2\sigma$  with respect to the SM expectation, as quoted in Table I, and it will be used in the combination. Besides the channel with at least 1SFOS lepton pair still makes use of the  $m_{\ell_0\ell_2}$  as the BDT input discriminating variable, as it can not be isolated and excluded to the  $Vh$  combination exercise. It is important to note that the 0SFOS category alone would provide a higher discrepancy, as in this case the  $H \rightarrow Sh$  is not expected to be rejected by the selection criteria. However, the previous statement is diluted in the observed signal strength result because both categories are combined in Ref. [18].

The CMS collaboration has also published results for the  $Vh$  production mode with  $h \rightarrow WW^*$  decay using Run 1 and partial Run 2 datasets [19, 20]. In these re-

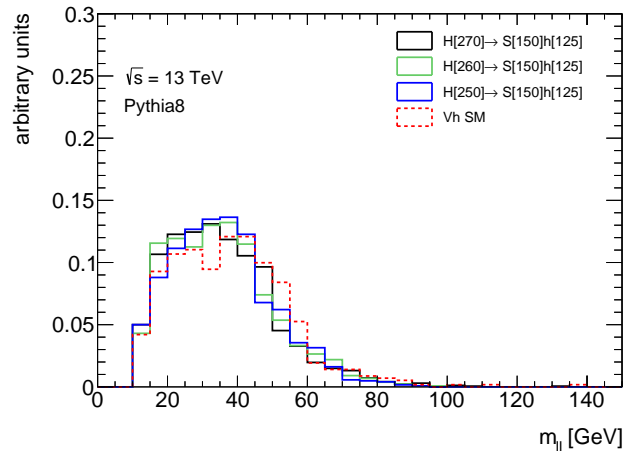


FIG. 2. Di-lepton invariant mass for several  $H \rightarrow Sh$  samples (solid lines) compared with the SM  $Vh$  process with  $h \rightarrow WW$  (dashed line) generated with PYTHIA8.

sults a  $Vh$  tagged category is defined by selecting events with a DFOS lepton pair with at least two jets in the final state. Similar to the ATLAS Run 1 strategy,  $m_{jj}$  is used to guarantee the consistency with the parent boson mass and  $|\Delta\eta_{jj}| < 3.5$  is applied to avoid overlap with VBF events. In addition, the leptons are required to have small  $\Delta R_{\ell\ell}$  since they are expected to be emitted in nearby directions due to the spin-0 nature of the SM Higgs boson. Finally,  $m_T$  is required to be between 60 GeV and the mass of the SM Higgs boson. The  $m_{\ell\ell}$  distribution is used as an input for the template fit to obtain the signal strength results. Both Run 1 and Run 2 results show a discrepancy between the observed data and the SM expectation at  $m_{\ell\ell} < 50$  GeV. The SM Higgs boson as well as the  $H \rightarrow Sh$  process are both expected to concentrate at the low  $m_{\ell\ell}$  region as shown in Figure 2. As quoted in Table I, the signal strength is below unity for the Run 1 analysis, while the observed Run 2 data presents an excess of  $\sim 3.4\sigma$ . Since the selection is the same in both cases there is no reason to select one result and reject the other. In light of the CMS event selection, the observed signal strengths from the DFOS category using Run 1 and Run 2 datasets will both be used in the combination.

Finally, CMS also targets events in the  $3\ell$  category which are further split into two channels depending on the existence of SFOS lepton pairs in the triplet. Opposite to ATLAS, the use of multivariate techniques is not considered by the CMS strategy, and specifically the  $|\sum p_T^{\ell_i}|$  variable is not used. To reduce Drell-Yan processes a lower bound on the  $E_T^{\text{miss}}$  and a  $Z$  boson veto are applied for 1SFOS events. The observed signal strength for this category is extracted using  $\Delta R_{\ell\ell}$  in the likelihood fit. Table I shows the same trend as previously discussed for the  $2\ell$  channel: Run 1 results present a signal strength below one but fully consistent with the SM due to the large uncertainty. The situation is the oppo-

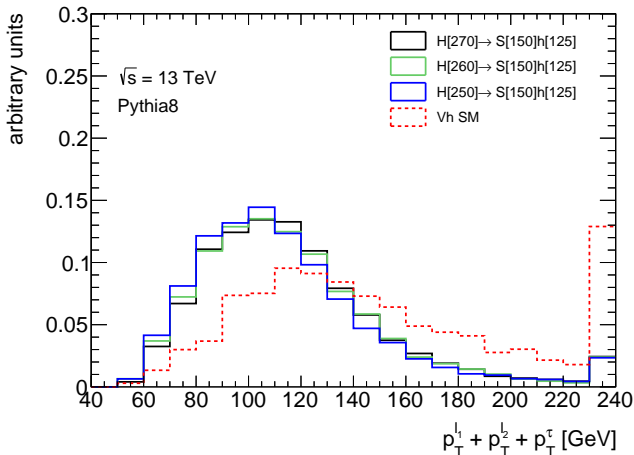


FIG. 3. Scalar sum of the transverse momentum of two leptons and a hadronic tau for several  $H \rightarrow Sh$  samples (solid lines) compared with the SM  $Vh$  process with  $h \rightarrow \tau\tau$  (dashed line) generated with PYTHIA8. The last bin contains overflow events.

site with the partial Run 2 dataset for which the signal strength is above unity, with a deviation from the SM expectation of  $\sim 1.3\sigma$ . As discussed for the  $2\ell$  category, both Run 1 and Run 2 results from CMS will be included in the combination.

### B. $Wh \rightarrow W\tau\tau$

Results for the associated production of the SM Higgs boson with a  $W$  boson, where the Higgs boson is decaying into a pair of tau leptons have been performed by the ATLAS and CMS collaborations. The strategy in both experiments split the events into two categories, depending on the number of tau leptons decaying to hadrons ( $\tau_{\text{had}}$ ), while the  $W$  boson is assumed to decay leptonically. In the first category, the selection requires one electron and one muon with the same electric charge; and the presence of one  $\tau_{\text{had}}$  candidate in the final state ( $e^\pm\mu^\pm\tau_{\text{had}}$ ). The second category selects events having one electron or muon accompanied by two  $\tau_{\text{had}}$  candidates from the SM Higgs decay ( $\ell\tau_{\text{had}}\tau_{\text{had}}$ ).

The results from ATLAS are obtained using the Run 1 dataset [21]. The kinematic selection for the  $e^\pm\mu^\pm\tau_{\text{had}}$  category requires the scalar sum of the  $p_T$  of the electron, muon and  $\tau_{\text{had}}$  to be greater than 80 GeV. As shown in Figure 3, this lower bound threshold keeps most of the  $Wh$  and  $H \rightarrow Sh$  processes. In the  $\ell\tau_{\text{had}}\tau_{\text{had}}$  category the transverse mass of the lepton and  $E_T^{\text{miss}}$  is required to be above 20 GeV and the two  $\tau_{\text{had}}$  candidates must be within a  $\Delta R$  of 2.8. Finally, the scalar sum of the  $p_T$  of the lepton and the two  $\tau_{\text{had}}$  is required to be above 100 GeV. Figure 4 compares the spectrum of this variable for both  $Wh$  and  $H \rightarrow Sh$  processes. Based on the kinematic selection used in these ATLAS Run 1 results, it is

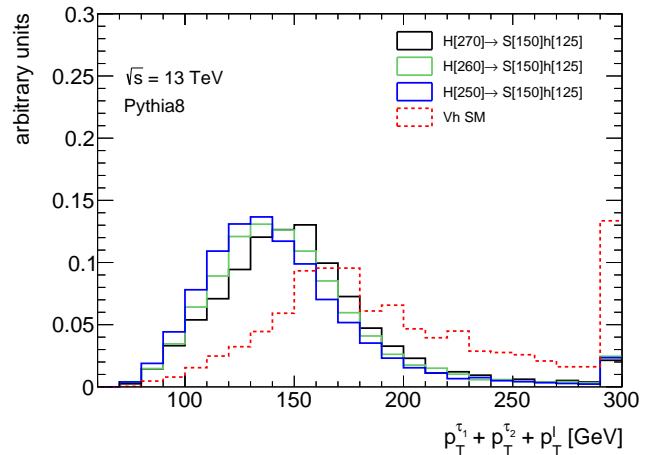


FIG. 4. Scalar sum of the of transverse momentum of the lepton and two hadronic taus for several  $H \rightarrow Sh$  samples (solid lines) compared with the SM  $Vh$  process with  $h \rightarrow \tau\tau$  (dashed line) generated with PYTHIA8. The last bin contains overflow events.

expected similar selection efficiencies for both  $Wh$  and  $H \rightarrow Sh$  processes, so these results will be used in the combination. The observed signal strength in each category is determined from a fit to the reconstructed Higgs boson candidate mass distribution, resulting in values above unity with relatively large uncertainties, as shown in Table I.

Results for the associated production with a  $W$  boson of the SM Higgs particle, when it decays to a pair of tau leptons, has been delivered by the CMS experiment using Run 1 and Run 2 data [19, 20]. However, the strategy and event selection is different for each dataset, and in the following they will be described. On the one hand, the  $\ell\tau_{\text{had}}\tau_{\text{had}}$  category in CMS Run 1 results makes use of a BDT discriminant based on the  $E_T^{\text{miss}}$  and on kinematics related to the di-tau system. One of the input discriminating variables is the ratio between the  $p_T$  of the two tau leptons over the scalar sum of their transverse momentum ( $p_T^{\tau_1} + p_T^{\tau_2}$ ). Figure 5 compares the  $p_T^{\tau_1} + p_T^{\tau_2}$  shapes for both  $Wh$  and  $H \rightarrow Sh$  processes. Given the main contribution for each case is located in different  $p_T^{\tau_1} + p_T^{\tau_2}$  regions, it is expected that the BDT discriminates the  $H \rightarrow Sh$  signal in benefit of the  $Wh$  process. On the other hand, the  $e^\pm\mu^\pm\tau_{\text{had}}$  category is further split into two by dividing the scalar sum of the leptons'  $p_T$  at 130 GeV. Figure 3 clearly shows that the contributions for each process in these two regions are inversely proportional. The likelihood fit is performed using the invisible mass of the Higgs decay lepton candidates in each  $p_T^e + p_T^\mu + p_T^\tau$  region. As a consequence of the different  $Wh$  and  $H \rightarrow Sh$  contributions shown in Figure 3, the statistical fit procedure tends to extract the  $Wh$  signal strength from the high region where it is dominant. The contribution from the BSM hypothesis is expected to not contribute significantly to these results

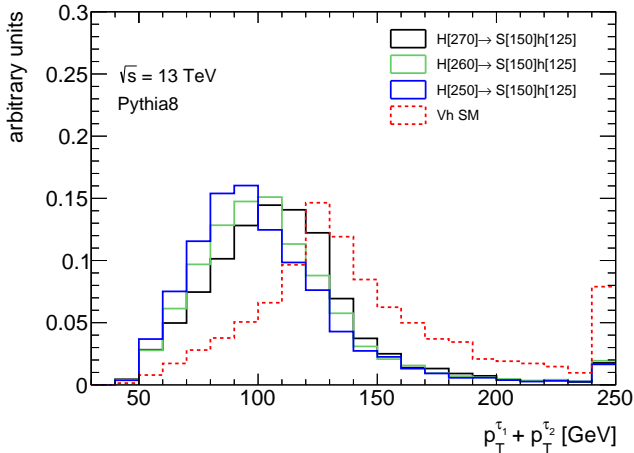


FIG. 5. Scalar sum of the transverse momentum of two hadronic taus for several  $H \rightarrow Sh$  samples (solid lines) compared with the SM  $Vh$  process with  $h \rightarrow \tau\tau$  (dashed line) generated with PYTHIA8. The last bin contains overflow events.

due to the selection criteria. In light of these features, the Run 1 results from CMS for the  $Wh$  with  $h \rightarrow \tau\tau$  are not considered for the signal strength combination in this paper.

The CMS strategy for the analysis of the Run 2 dataset follows a different approach. The category with one  $\tau_{\text{had}}$  in the final state requires the scalar sum of the  $p_T$  of the leptons and the  $\tau_{\text{had}}$  to be above 100 GeV. From Figure 3 it can be seen that the  $H \rightarrow Sh$  efficiency after this cut is applied is above 70%. Since the Higgs and  $W$  bosons are dominantly produced back-to-back in  $\phi$ , and they may have a longitudinal Lorentz boost, that makes them close in  $\eta$ . As such, two angular separation cuts between the highest  $p_T$  lepton and the system formed by the  $\tau_{\text{had}}$  and the remaining lepton are applied. In the  $\ell\tau_{\text{had}}\tau_{\text{had}}$  category, the threshold on the scalar sum of the lepton and the two  $\tau_{\text{had}}$  is 130 GeV. As shown in Figure 4, this cut still keeps about 60% of the  $H \rightarrow Sh$  process. In addition, the vectorial sum of  $p_T$  of the lepton, the two  $\tau_{\text{had}}$  candidates and the  $E_T^{\text{miss}}$  is required to be below 70 GeV. Finally, only events with small angular separation of the two  $\tau_{\text{had}}$  candidates in  $\eta$  are selected. Given the fact that the event selection is not expected to affect the  $H \rightarrow Sh$  efficiency dramatically, this result should be used in the combination. The observed signal strength for this case presents a deviation with respect to the SM expectation of about  $2\sigma$ , as shown in Table I.

### C. $Wh \rightarrow W\gamma\gamma$

Results for the associated production of a  $W/Z$  boson with the SM Higgs particle when it decays into a pair of photons have also been released by the ATLAS and CMS collaborations using both Run 1 and partial Run 2 datasets [24–27]. The selection criteria in both cases

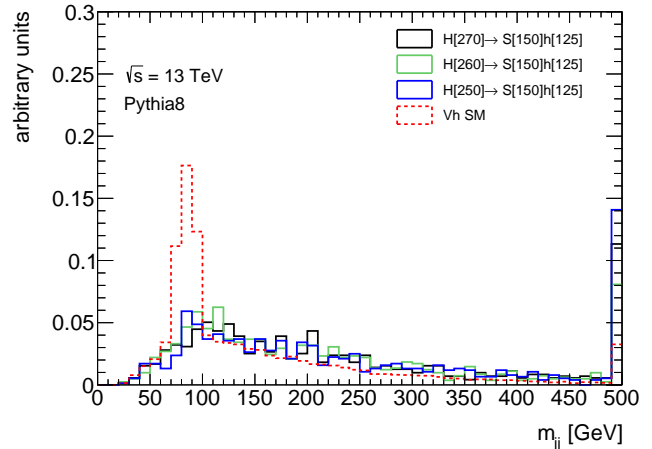


FIG. 6. Dijet invariant mass in events with two photons and at least two jets for several  $H \rightarrow Sh$  samples (solid lines) compared with the SM  $Vh$  process with  $h \rightarrow \gamma\gamma$  (dashed line) generated with PYTHIA8. The last bin contains overflow events.

exploits the presence of leptons, jets and  $E_T^{\text{miss}}$ , hence the events are classified into three main categories:  $Wh$  one-lepton,  $Vh$  hadronic and  $Vh E_T^{\text{miss}}$ .

Events in the  $Vh$  hadronic category are required to have a pair of two high-energy jets originating from the vector boson decay, hence with  $m_{jj}$  consistent with the  $V$  boson mass. Figure 6 compares the invariant mass of the dijet system for the SM Higgs boson associated production and the  $H \rightarrow Sh$  process. For the  $Wh$  process the efficiency reaches more than 50% when selecting an  $m_{jj}$  window cut in the range of [60 – 120] GeV. For the BSM process of interest here, the  $m_{jj}$  selection keeps around 20% of the total statistics. Results from CMS make use of the angle between the diphoton and the diphoton-dijet system in both Run 1 and Run 2 datasets. The difference between both CMS strategies is the  $p_T^{\gamma\gamma} > 13m_{\gamma\gamma}/12$  requirement, which is only applied in the Run 1 case. Figure 7 shows the ratio between the diphoton transverse momentum and its invariant mass. The  $13p_T^{\gamma\gamma} > m_{\gamma\gamma}/12$  requirement highly reduces the  $H \rightarrow Sh$  acceptance by rejecting more than 85% of the BSM events. In light of this, the CMS Run 1 results will not be used for the combination while the Run 2 can be used as the later analysis does not rely on the  $p_T^{\gamma\gamma}/m_{\gamma\gamma}$  variable. From Ref. [27], the Run 2 CMS results for this category present a deviation from the SM expectation of approximately  $2.2\sigma$ , being the measured signal strength  $5.1_{-2.3}^{+2.5}$ .

ATLAS uses the magnitude of the component of the diphoton momentum transverse to its thrust axis in the transverse plane ( $p_{Tt}^{\gamma\gamma}$ ). In Run 1 analysis the  $m_{jj}$  must be in the range 60 – 110 GeV and the  $p_{Tt}^{\gamma\gamma}$  is required to be above 70 GeV. In Run 2 a BDT with  $m_{jj}$  and  $p_{Tt}^{\gamma\gamma}$  input variables are used to discriminate the  $Vh$  process.

The  $Vh E_T^{\text{miss}}$  category is enriched in events with a leptonic decay of the  $W$  boson, when the lepton is not

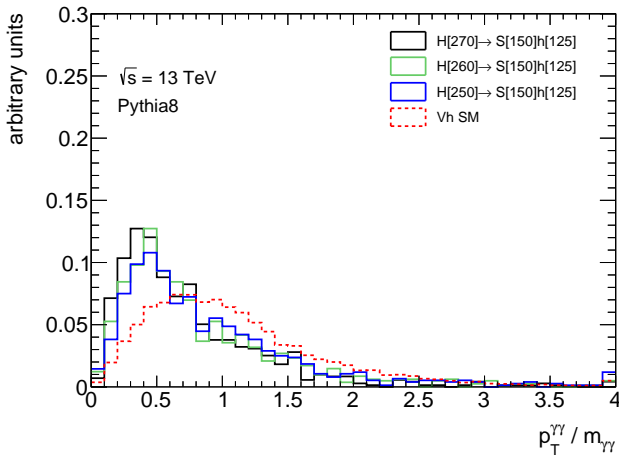


FIG. 7. Ratio between the transverse momentum and the invariant mass of the diphoton system in events with at least two jets for several  $H \rightarrow Sh$  samples (solid lines) compared with the SM  $Vh$  process with  $h \rightarrow \gamma\gamma$  (dashed line) generated with PYTHIA8. The last bin contains overflow events.

detected or does not satisfy the selection criteria (denoted by  $\cancel{\ell}$ ), or with a  $Z$  boson decaying into a pair of neutrinos. In this case the selection criteria relies on the  $E_T^{\text{miss}}$  distribution to select events in the high range. The strategy from CMS uses a lower bound of 85(70) GeV on the  $E_T^{\text{miss}}$  for Run 2(1) results. Similarly, ATLAS Run 1 results are obtained by applying a cut on a  $E_T^{\text{miss}}$  based quantity which is roughly equivalent to a direct requirement of  $E_T^{\text{miss}} > 70 - 100$  GeV. Finally, in ATLAS Run 2 results this category is further split into two: one requiring  $80 < E_T^{\text{miss}} < 150$  GeV and the other with  $E_T^{\text{miss}} > 150$  GeV cut. Given the high thresholds applied on the  $E_T^{\text{miss}}$ , this category will not be used for the combination.

The  $Wh$  one-lepton class is characterized by a leptonically decaying  $W$  boson, hence it targets events with two photons accompanied with one electron or one muon. In the Run 2 strategy the events in ATLAS are split using the transverse momentum of the lepton and the  $E_T^{\text{miss}}$  ( $p_T^{l+E_T^{\text{miss}}}$ ) at 150 GeV. Figure 8 compares the shape of the  $p_T^{l+E_T^{\text{miss}}}$  quantity for  $Wh$  and  $H \rightarrow Sh$  processes. The high region of the distribution is expected to contribute more in the likelihood fit, since there the SM backgrounds are expected to be significantly smaller. This behavior enhances the  $Wh$  signal over the background ratio. The BSM process is mostly uniquely located at  $p_T^{l+E_T^{\text{miss}}} < 150$  GeV, so its contribution could be diluted in the region where the SM backgrounds are expected to dominate. The ATLAS strategy for the Run 1 dataset selects  $Wh$  one-lepton events by applying a cut on a  $E_T^{\text{miss}}$  related quantity. CMS also further splits the one-lepton category by dividing the  $E_T^{\text{miss}}$  spectrum at 45 GeV. Figure 9 shows the missing transverse energy for events with two photons and a lepton. At this cut value,

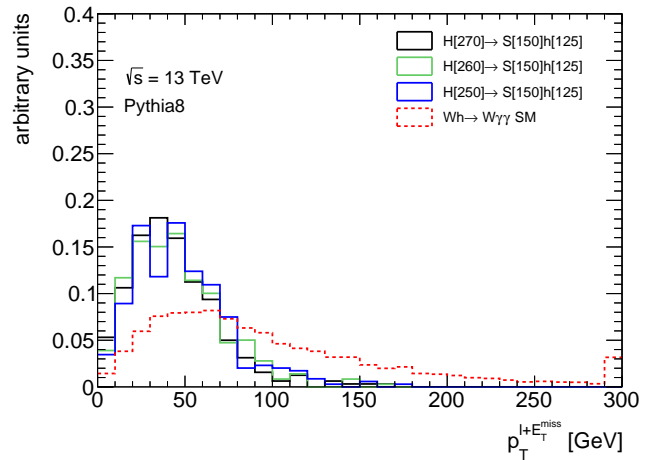


FIG. 8. Transverse momentum of the lepton and the  $E_T^{\text{miss}}$  system in events with two photons and a lepton for several  $H \rightarrow Sh$  samples (solid lines) compared with the SM  $Wh$  process with  $h \rightarrow \gamma\gamma$  (dashed line) generated with PYTHIA8. The last bin contains overflow events.

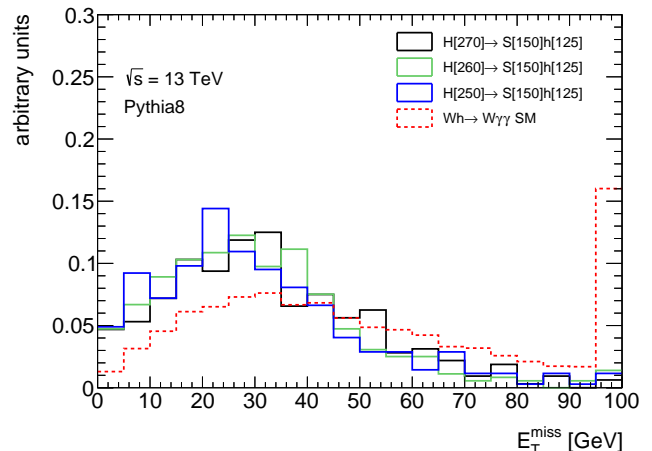


FIG. 9. Missing transverse energy in events with two photons and one electron or muon for several  $H \rightarrow Sh$  samples (solid lines) compared with the SM  $Wh$  process with  $h \rightarrow \gamma\gamma$  (dashed line) generated with PYTHIA8. The last bin contains overflow events.

the  $Wh$  process is divided by 50% in each region, being the events in the high  $E_T^{\text{miss}}$  range and the ones driving the result on the measured signal strength, as discussed above for the case of the  $p_T^{l+E_T^{\text{miss}}}$ . The  $H \rightarrow Sh$  signal acceptance is approximately 20% in the high  $E_T^{\text{miss}}$  region.

The CMS Run 1 results will be discarded in the combination as they are computed including not only the  $Vh$  one-lepton category but also the hadronic and  $E_T^{\text{miss}}$  ones as well. Conversely, CMS Run 2 results are produced in the Higgs simplified template cross section framework and delivered for the one-lepton and the hadronic categories separately. Aside from the same strategy being

adopted with Run 1 and Run 2 datasets for CMS, we can only consider the later set of results as the measured signal strengths are provided for each analysis category. The Run 2 CMS result shows a deviation from the SM expectation of around  $2\sigma$ . The observed signal strength of the  $Wh$  one-lepton category is  $3.0_{-1.3}^{+1.5}$  and will be used in the combination.

#### IV. RESULTS AND CONCLUSIONS

The interpretation of the multi-lepton anomalies at the LHC reported in Refs. [1, 2] with the decay  $H \rightarrow Sh$  predicts anomalously large values of the signal strength of  $Wh$ . This effect should be visible with the available results from ATLAS and CMS so far.

Section III provides a comprehensive synopsis of the current status of the search and measurements of  $Wh$  production in the SM, where the available results correspond to the Run 1 and about one fourth of the Run 2 data sets. Table I gives the summary of the available results and indicates which ones are used in the combination with the appropriate explanation. The overall combination of the results excluding those discarded in Table I is  $\mu(Wh)_{Inc} = 2.51 \pm 0.43$ . This corresponds to a deviation from the SM value of unity of  $3.5\sigma$ . As discussed in Section III, the estimate made here is based on searches and measurements biased towards the SM. Therefore, the true deviation from unity is likely to be larger.

The impact on the measurement of  $h$ -related cross-sections due to the BSM signal considered here goes beyond the associated production of leptons, as discussed here. The measurement of the Higgs boson transverse momentum and rapidity will also be affected. These effects will be studied with results with the full Run 2 data set, when available.

While the effect seen here seems in qualitative agreement with the multi-lepton anomalies interpreted with the simplified model described in Section II, it is important to confront the value of  $\mu(Wh)_{Inc}$  with that expected with the ansatz of  $\text{Br}(H \rightarrow Sh) = 100\%$  made in Refs. [1, 2]. Assuming the cross-section  $\sigma(H \rightarrow S^*h) = 10 \text{ pb}$ , where  $h$  is on-shell, one would expect a combined (including the SM) signal strength of about 6 for the combination of the channels considered in Section III. This is considerably larger than the signal strength observed here, notwithstanding the expected bias discussed in Sec-

tion III. This indicates that explaining the multi-lepton anomalies reported in Refs. [1, 2] would require a considerable contribution from  $H \rightarrow SS$  along with  $H \rightarrow Sh$ . The decay  $H \rightarrow hh$  would be suppressed due to results from direct searches.

The emergence of anomalously large production of  $h$  in association with leptons gives further credence to the possible connection of the multi-lepton anomalies at the LHC with new physics around the EW scale. The excesses reported here sit in different corners of the phase-space where the decays of  $h$  are relevant, as opposed to the final states considered in Refs. [1, 2]. The results of this paper further enriches the plethora of multi-lepton anomalies observed at the LHC.

Irrespective of the size of  $\mu(Wh)_{Inc}$  determined here, one needs to seriously consider a situation whereby the production of  $h$  at the LHC is contaminated with production mechanisms other than those predicted in the SM. This implies that the determination of couplings of  $h$  to SM particles would be seriously compromised by model dependences. This further enhances the physics case of Higgs factories on the basis of  $e^+e^-$  [30–32] and  $e^-p$  [33–35] collisions, while the potential for the direct observation of new physics at the HL-LHC is enriched strongly. The production of  $H$  in  $e^-p$  collisions would be suppressed, therefore, the determination of the Higgs boson couplings would be less model dependent compared to proton-proton collisions. Assuming the current value of the  $h$  global signal strength at the LHC,  $\mu(h) = 1.133 \pm 0.054(\text{exp.})$ , and that the couplings of  $h$  to SM particles are as in the SM, the contamination at the LHeC would be five times smaller than that at the LHC [36]. The LHeC, with input from proton-proton collisions, would allow for the precise determination of the  $hWW$  coupling, which combined with the superb measurement of the  $hZZ$  coupling in  $e^+e^-$  collisions, would provide a powerful probe into Electro-Weak Symmetry breaking.

#### V. ACKNOWLEDGEMENTS

The authors are grateful for support from the South African Department of Science and Innovation through the SA-CERN program and the National Research Foundation for various forms of support. The authors are also indebted to the Research Office of the University of the Witwatersrand for grant support.

- 
- [1] S. von Buddenbrock, A. S. Cornell, A. Fadol, M. Kumar, B. Mellado and X. Ruan, *J. Phys. G* **45**, no. 11, 115003 (2018) [arXiv:1711.07874 [hep-ph]].
  - [2] S. Buddenbrock, A. S. Cornell, Y. Fang, A. Fadol Mohammed, M. Kumar, B. Mellado and K. G. Tomiwa, *JHEP* **1910**, 157 (2019) [arXiv:1901.05300 [hep-ph]].
  - [3] P. W. Higgs, *Phys. Lett.* **12**, 132 (1964).
  - [4] F. Englert and R. Brout, *Phys. Rev. Lett.* **13**, 321 (1964).
  - [5] P. W. Higgs, *Phys. Rev. Lett.* **13**, 508 (1964).
  - [6] G. S. Guralnik, C. R. Hagen and T. W. B. Kibble, *Phys. Rev. Lett.* **13**, 585 (1964).
  - [7] G. Aad *et al.* [ATLAS Collaboration], *Phys. Lett. B* **716**, 1 (2012) [arXiv:1207.7214 [hep-ex]].

- [8] S. Chatrchyan *et al.* [CMS Collaboration], Phys. Lett. B **716**, 30 (2012) [arXiv:1207.7235 [hep-ex]].
- [9] S. Chatrchyan *et al.* [CMS Collaboration], Phys. Rev. Lett. **110**, no. 8, 081803 (2013) [arXiv:1212.6639 [hep-ex]].
- [10] G. Aad *et al.* [ATLAS Collaboration], Phys. Lett. B **726**, 120 (2013) [arXiv:1307.1432 [hep-ex]].
- [11] S. von Buddenbrock *et al.*, arXiv:1506.00612 [hep-ph].
- [12] S. von Buddenbrock *et al.*, Eur. Phys. J. C **76**, no. 10, 580 (2016) [arXiv:1606.01674 [hep-ph]].
- [13] S. von Buddenbrock, A. S. Cornell, E. D. R. Iarilala, M. Kumar, B. Mellado, X. Ruan and E. M. Shrif, J. Phys. G **46**, no. 11, 115001 (2019) [arXiv:1809.06344 [hep-ph]].
- [14] S. von Buddenbrock and B. Mellado, arXiv:1909.04370 [hep-ph].
- [15] S. von Buddenbrock, J. Phys. Conf. Ser. **878**, no. 1, 012030 (2017) [arXiv:1706.02477 [hep-ph]].
- [16] Y. Fang, M. Kumar, B. Mellado, Y. Zhang and M. Zhu, Int. J. Mod. Phys. A **32**, no. 34, 1746010 (2017) [arXiv:1706.06659 [hep-ph]].
- [17] ATLAS Collaboration, JHEP **08** (2015) 137, [arXiv:1506.06641 [hep-ex]].
- [18] ATLAS Collaboration, Phys. Lett. B **798** (2019) 134949, [arXiv:1903.10052 [hep-ex]].
- [19] CMS Collaboration, JHEP **01** (2014) 096, [arXiv:1312.1129 [hep-ex]].
- [20] CMS Collaboration, Phys. Lett. B **791** (2019) 96, [arXiv:1806.05246 [hep-ex]].
- [21] ATLAS Collaboration, Phys. Rev. D **93**, 092005 (2016), [arXiv:1511.08352 [hep-ex]].
- [22] CMS Collaboration, JHEP **05** (2014) 104, [arXiv:1401.5041 [hep-ex]].
- [23] CMS Collaboration, JHEP **06** (2019) 093, [arXiv:1809.03590 [hep-ex]].
- [24] ATLAS Collaboration, Phys. Rev. D **90**, 112015 (2014), [arXiv:1408.7084 [hep-ex]].
- [25] CMS Collaboration, Phys. Rev. D **98** (2018) 052005, [arXiv:1802.04146 [hep-ex]].
- [26] ATLAS Collaboration, Eur. Phys. J. C **74** (2014) 3076, [arXiv:1407.0558 [hep-ex]].
- [27] CMS Collaboration, JHEP **11** (2018) 185, [arXiv:1804.02716 [hep-ex]].
- [28] A. Hoecker *et al.*, CERN-OPEN-2007-007, [arXiv:physics/0703039 [physics.data-an]].
- [29] F. Predregosa *et al.*, Journal of Machine Learning Research (2011), [arXiv:1201.0490 [cs.LG]].
- [30] H. Baer *et al.*, arXiv:1306.6352 [hep-ph].
- [31] J. B. Guimarães da Costa *et al.* [CEPC Study Group], arXiv:1811.10545 [hep-ex].
- [32] A. Abada *et al.* [FCC Collaboration], Eur. Phys. J. ST **228**, no. 2, 261 (2019).
- [33] J. L. Abelleira Fernandez *et al.* [LHeC Study Group], J. Phys. G **39**, 075001 (2012) [arXiv:1206.2913 [physics.acc-ph]].
- [34] T. Han and B. Mellado, Phys. Rev. D **82**, 016009 (2010) [arXiv:0909.2460 [hep-ph]].
- [35] S. S. Biswal, R. M. Godbole, B. Mellado and S. Raychaudhuri, Phys. Rev. Lett. **109**, 261801 (2012) [arXiv:1203.6285 [hep-ph]].
- [36] C. Mosomane, M. Kumar, A. S. Cornell and B. Mellado, J. Phys. Conf. Ser. **889**, no. 1, 012004 (2017) [arXiv:1707.05997 [hep-ph]].